

Analogy between rotation and density for Dirac fermions in a magnetic field

Hao-Lei Chen,¹ Kenji Fukushima,² Xu-Guang Huang,¹ and Kazuya Mameda²

¹*Physics Department and Center for Particle Physics and Field Theory, Fudan University, Shanghai 200433, China*

²*Department of Physics, The University of Tokyo, Tokyo 113-0033, Japan*

We analyse the energy spectra of Dirac fermions in the presence of rotation and magnetic field. We find that the Landau degeneracy is resolved by rotation. A drastic change in the energy dispersion relation leads to the “rotational magnetic inhibition” that is a novel phenomenon analogous to the inverse magnetic catalysis in a magnetic system at finite chemical potential.

PACS numbers: 04.62.+v, 11.30.Rd, 21.65.Qr

I. INTRODUCTION

In many quantum theories an external magnetic field is a useful probe for various intriguing phenomena. The most important concept to understand the magnetic dynamics appears from the Landau quantization. For a strong enough magnetic field only the lowest Landau level (LLL) dominates the dynamics. Such a situation with a gigantic magnetic field could be realized in the Early Universe [1, 2] and in central cores of neutron stars (or magnetars) where $eB \sim 10^{15}$ G [3]. Also, an extreme environment with a strong magnetic field could be generated in relativistic heavy-ion collision experiments where we may have $eB \sim m_\pi^2 \sim 10^{18}$ G [4–6]. Investigating quantum chromodynamics (QCD) in a strong magnetic field is, therefore, of increasing importance for not only theoretical interest but also experimental application [7]. In particular the response of quark matter to the magnetic field involves \mathcal{P} - and \mathcal{CP} -odd processes through quantum anomaly, which is still under active studies [8–12] (see also Refs. [13] as related reviews).

One of the most essential and established changes of quark matter driven by strong magnetic fields is the inevitable breaking of chiral symmetry, which is called the magnetic catalysis [14–16]. We can confirm the magnetic catalysis in many theoretical examples which include: the Nambu–Jona-Lasinio (NJL) model [15, 17, 18], the quark-meson model [19–22], the MIT bag model [23], the lattice QCD simulation [24], the holographic model [25] (see also Refs. [16] for reviews and the references therein). The idea of charged particles acquiring a dynamical mass due to the magnetic field is applicable also to condensed matter systems such as the graphene [26], the Weyl semimetals [27], and bosonic systems [28, 29].

The magnetic catalysis could be affected by other controlling parameters even though the magnetic field is strong. For instance, in a dense system at large chemical potential, the magnetic field would not enhance but suppress the chiral condensate, which is called the inverse magnetic catalysis [17, 30]. Inclusion of neutral meson fluctuations could lead to an infrared singularity that disfavors the chiral condensate, which is called the magnetic inhibition [31]. In this way it would be useful to consider magnetic systems under competing conditions for drawing further nontrivial consequences from the physics of

the magnetic catalysis [32–35].

In this work we will pay attention to the competition between rotation and the magnetic catalysis. It is well known that the effect of rotation or angular momentum is quite analogous to that of the magnetic field. Especially for nonrelativistic systems in a trapping potential one can show that the system exhibits the Landau-type quantization in response to rotation [36, 37]. This analogy has motivated people to study anomalous quantum phenomena induced by rotation instead of magnetic field, that is, the quantum Hall effect induced by rotation [38], the quantum vortex with rotating Bose-Einstein condensate [39], the chiral vortical effect [11], and the chiral magnetic effect in cold atoms [40].

We would emphasize another interesting (and less known) analogy between rotation and density. For non-relativistic theories this analogy is readily understood from the fact that the Hamiltonian in a rotating frame is shifted as $\hat{H} \rightarrow \hat{H} - \hat{\mathbf{L}} \cdot \boldsymbol{\Omega}$ (with the angular velocity vector $\boldsymbol{\Omega}$) and this latter term may be regarded as an effective chemical potential. One might thus expect that the similarity between rotation and density should hold for relativistic theories. However, the similarity in the relativistic case is, if any, not as trivial because one should treat relativistic rotation as a deformation of spacetime geometry. That means, to study rotational effects on relativistic systems, it is necessary to analyse the quantum field theory in curved spacetime [41]. (Also from the viewpoint of the Poincaré algebra, rotating relativistic fluid can be discussed [42, 43].) Although QCD in curved spacetime is not yet a mature research subject and not much about modified QCD vacuum structure is known, it has been argued that the gravitational background fields should significantly influence the QCD vacuum properties [44–47] (see also Refs. [48–50] for quantum lattice simulations). It is, therefore, an intriguing question that whether rotation could be given an interpretation as an effective chemical potential even for relativistic theories. If so, rotation should yield a modification on the QCD vacuum and, particularly in the presence of strong magnetic field, we may anticipate an effect analogous to the inverse magnetic catalysis in which the role played by the chemical potential is replaced with rotation. We would call the phenomenon of reduced chiral condensate by a combination of rotation and magnetic field the “rota-

tional magnetic inhibition" in short.

In this paper, we investigate the Dirac equation with both rotation and magnetic field and apply the resulting energy dispersion relation to a fermionic effective model. The solution of the Dirac equation indicates that the modified Landau levels with rotation have nondegenerate spectrum with angular momentum dependence. We adopt the NJL model and impose both the magnetic field and rotation to find chiral restoration that is driven by increasing magnetic field especially at strong coupling. Finally we will discuss possible physical implications of our results to several experimental setups.

II. DIRAC EQUATION IN A ROTATING FRAME

In curved spacetime generally the Dirac equation with electromagnetic fields can be written as

$$[i\gamma^\mu(D_\mu + \Gamma_\mu) - m]\psi = 0 \quad (1)$$

with the covariant derivative $D_\mu \equiv \partial_\mu + ieA_\mu$ and $e > 0$ being the charge of the Dirac fermion. As usual, the affine connection Γ_μ is defined in terms of the metric $g_{\mu\nu}$ or the spin connection $\omega_{\mu ij}$ and the vierbein e_i^μ as

$$\begin{aligned} \Gamma_\mu &= -\frac{i}{4}\omega_{\mu ij}\sigma^{ij}, \\ \omega_{\mu ij} &= g_{\alpha\beta}e_i^\alpha(\partial_\mu e_j^\beta + \Gamma_{\mu\nu}^\beta e_j^\nu), \\ \sigma^{ij} &= \frac{i}{2}[\gamma^i, \gamma^j]. \end{aligned} \quad (2)$$

The Greek and the Latin letters denote the indices in coordinate and tangent space, respectively.

We can implement rotation by specifying the metric characterized by the angular velocity vector, $\boldsymbol{\Omega} = \Omega\hat{z}$, and the metric then takes the following form:

$$g_{\mu\nu} = \begin{pmatrix} 1 - (x^2 + y^2)\Omega^2 & y\Omega & -x\Omega & 0 \\ y\Omega & -1 & 0 & 0 \\ -x\Omega & 0 & -1 & 0 \\ 0 & 0 & 0 & -1 \end{pmatrix}. \quad (3)$$

In the following calculation we adopt

$$e_0^t = e_1^x = e_2^y = e_3^z = 1, \quad e_0^x = y\Omega, \quad e_0^y = -x\Omega, \quad (4)$$

and the other components are zero, which gives the metric (3). We shall choose the symmetric gauge in the inertial frame and use the vector potential, $A_i = (0, By/2, -Bx/2, 0)$, which results in $\mathbf{B} = B\hat{z}$ with B a constant. We can then give an explicit form of the Dirac equation under rotation and the magnetic field, that is,

$$\begin{aligned} &[i\gamma^0(\partial_t - x\Omega\partial_y + y\Omega\partial_x - i\Omega\sigma^{12}) + i\gamma^1(\partial_x + ieBy/2) \\ &+ i\gamma^2(\partial_y - ieBx/2) + i\gamma^3\partial_z - m]\psi = 0. \end{aligned} \quad (5)$$

We can solve this differential equation to obtain the wavefunction as explained in Appendix A. For our purpose to study the vacuum structure, we do not need the wavefunction but only the energy spectrum is sufficient.

It is easy to deduce the eigen-energies of Eq. (5) at finite Ω from the $\Omega = 0$ case. In this case the problem is reduced to solving the ordinary Dirac equation in an external magnetic field. It is a well-known fact that charged spin- s particles have the energy dispersion relation in $\mathbf{B} = B\hat{z}$ ($eB > 0$) as

$$E^2 = p_z^2 + (2n + 1 - 2s_z)eB + m^2 \quad (6)$$

with non-negative integer n . Compared with that without rotation, the Dirac equation (5) with rotation has additional pieces of

$$-i(x\Omega\partial_y + y\Omega\partial_x) + \Omega\sigma^{12} = \Omega(\hat{L}_z + \hat{S}_z). \quad (7)$$

We denote the eigenvalues for \hat{L}_z and \hat{S}_z as ℓ and s_z , respectively. We can regard $E + \Omega(\ell + s_z)$ as the energy eigenvalue in the inertial frame. In this way we can reach the expression of the energy dispersion relations from Eq. (5) given by

$$[E + \Omega(\ell + s_z)]^2 = p_z^2 + (2n + 1 - 2s_z)eB + m^2. \quad (8)$$

In what follows we discuss some features of Dirac fermions in a rotating frame.

(I) First, we make a comment on the Lorentz force in a rotating frame. The gauge fields are transformed in a rotating frame into the following form:

$$A_\mu = A_i e_\mu^i = (-B\Omega r^2/2, By/2, -Bx/2, 0), \quad (9)$$

which leads to an electric field; $\mathbf{E} = -\nabla A_0 = B\Omega(x, y, 0)$. Hence, naively, one may want to identify this \mathbf{E} as the Lorentz force:

$$\mathbf{F} = e\mathbf{v} \times \mathbf{B} = eB\Omega(x, y, 0), \quad (10)$$

where $\mathbf{v} = \Omega(-y, x, 0)$ is the velocity vector at $(x, y, 0)$ caused by rotation. However, $A_0 = -B\Omega r^2/2$ does not appear in Eq. (5) because the gamma matrix $\gamma^t = \gamma^i e_i^t$ cancels it out. Therefore, rotation does not induce any electromagnetic effect. This is an important point that ensures our later discussion on the similarity between rotation and finite density for relativistic theories.

(II) Let us take a closer look at the comparison of Eqs. (6) and (8). Without rotation, Eq. (6) expresses the ordinary Landau quantization in which the motion on the xy -plane is characterized by n only instead of (p_x, p_y) . Each Landau level has degeneracy associated with some quantum number; when the area of the xy -plane is S , the degeneracy factor for each Landau level is gauge independent and given by

$$N = \left\lfloor \frac{eBS}{2\pi} \right\rfloor. \quad (11)$$

In the cylindrical coordinates, for example, the degenerate quantum number is the canonical angular momentum ℓ . Thus, ℓ should take N different integers. In addition, a condition, $\ell \geq -n$ for the n th Landau level arises from normalizability of the wave-function. It follows that the possible range of ℓ should be

$$-n \leq \ell \leq N - n \quad (12)$$

for the n th Landau level. We give a detailed derivation for this in Appendix B. (One might think that ℓ should run up to $N - n - 1$ but we implicitly assume $N \gg 1$ with sufficiently strong magnetic field.)

The angular momentum in Eq. (8) also runs from $-n$ to $N - n$ (see Appendix A for details). This means that we have nondegenerate spectrum depending on ℓ in Eq. (8). We should replace the phase space integration with double sum with respect to n and ℓ . For spin-1/2 fermions with up spin, the phase space sum reads:

$$\begin{aligned} \text{Magnetic field: } \int \frac{dp_x dp_y}{(2\pi)^2} &\rightarrow \frac{eB}{2\pi} \sum_{n=0}^{\infty}, \\ \text{Magnetic field + Rotation: } \int \frac{dp_x dp_y}{(2\pi)^2} &\rightarrow \frac{1}{S} \sum_{n=0}^{\infty} \sum_{\ell=-n}^{N-n}, \end{aligned} \quad (13)$$

where N is the Landau degeneracy factor given in Eq. (11). This modified phase space sum is needed for the evaluation of the thermodynamic potential.

(III) The analogy between rotation and density is clear from Eq. (8). The dispersion relation (8) behaves as if the Dirac fermion were put at finite density with a chemical potential $\mu_j = \Omega j \equiv \Omega(\ell + s_z)$. Note that due to this similarity, the Dirac fermions under rotation also suffer from the sign problem for Monte Carlo simulations [48]. In this paper, motivated by such a similarity, we study a relativistic many-body system with rotation and magnetic field. In the next section we will show that rotation may supersede the magnetic catalysis.

(IV) Finally, we address the necessary condition for the system size. For quantization in harmonic oscillators, the system size should be large enough as compared to typical scales of the problem. In order to discuss the Landau quantization in the cylindrical system with area $S = \pi R^2$, hence, the radius R should be larger than the magnetic length, $\ell_B = 1/\sqrt{eB}$ (see Appendix A). In the rest frame we have no problem taking such a large cylinder toward the thermodynamic limit, i.e. $R \rightarrow \infty$. Once rotation is involved, however, the system with infinitely large radius is not well-defined because the causality might be violated at the edges of the cylinder where $R\Omega \geq 1$ [51, 52]. Therefore, our treatment in this paper is legitimate if R is not too small to justify the quantization, and not too large to maintain the causality. That is, the following condition should be imposed:

$$1/\sqrt{eB} \ll R \leq 1/\Omega. \quad (14)$$

We note that $N \gg 1$ follows from the above condition.

III. NJL MODEL WITH ROTATION AND MAGNETIC FIELD

We investigate the dynamical breaking of chiral symmetry in the presence of rotation and magnetic field using the NJL model [53], which is defined in curved spacetime by

$$\begin{aligned} S &= \int d^4x \sqrt{-\det(g_{\mu\nu})} \mathcal{L}(\bar{\psi}, \psi), \\ \mathcal{L} &= \bar{\psi} [i\gamma^\mu (D_\mu + \Gamma_\mu) - m_{\text{current}}] \psi \\ &\quad + \frac{G}{2} [(\bar{\psi}\psi)^2 + (\bar{\psi}\gamma_5\psi)^2]. \end{aligned} \quad (15)$$

Here, $\det(g_{\mu\nu}) = -1$ for the metric (3) and G denotes the coupling constant. In the usual way we can introduce auxiliary fields and utilize the mean-field approximation to obtain the effective thermodynamic potential:

$$\begin{aligned} V_{\text{eff}}(m) &= \frac{(m - m_{\text{current}})^2}{2G} - \frac{T}{S} \sum_{q=\pm} \int_{-\infty}^{\infty} \frac{dp_z}{2\pi} \sum_{n,\ell,s_z} \\ &\quad \times \left\{ \frac{\beta(\varepsilon + q\Omega j)}{2} + \ln[1 + e^{-\beta(\varepsilon + q\Omega j)}] \right\}, \end{aligned} \quad (16)$$

where ε is the energy dispersion relation without rotation, i.e. $\varepsilon \equiv \sqrt{p_z^2 + (2n + 1 - 2s_z)eB + m^2}$. The effective potential (16) is the same as that at finite density once Ωj is identified as a constant chemical potential μ [17]. We should note that we implicitly assume a spatially homogeneous chiral condensate so that the dynamical mass in the energy dispersion relation takes an ordinary form. At zero temperature, particularly, we can decompose Eq. (16) into the pure-magnetic and rotational contributions as

$$V_{\text{eff}}(m) = \frac{(m - m_{\text{current}})^2}{2G} + V_0 + V_\Omega, \quad (17)$$

where

$$V_0 = -\frac{eB}{2\pi} \sum_{n=0}^{\infty} \alpha_n \int_{-\infty}^{\infty} \frac{dp_z}{2\pi} \sqrt{p_z^2 + m_n^2}, \quad (18)$$

and

$$\begin{aligned} V_\Omega &= -\frac{1}{S} \sum_{n=0}^{\infty} \alpha_n \sum_{\ell=-n}^{N-n} \theta(\Omega|j| - m_n) \\ &\quad \times \int_{-k_{nj}}^{k_{nj}} \frac{dp_z}{2\pi} [\Omega|j| - \sqrt{p_z^2 + m_n^2}] \end{aligned} \quad (19)$$

with $j = \ell + 1/2$ hereafter and $\Omega > 0$. Here, we introduced the following notations: $\alpha_n = 2 - \delta_{n0}$, $m_n^2 = 2neB + m^2$, and $k_{nj} \equiv \sqrt{(\Omega j)^2 - m_n^2}$.

Now we must specify the ultraviolet regularization scheme needed for Eq. (17). The NJL model is not

renormalizable, and so the regularization scheme is a part of the model definition. Without electromagnetic background fields, a sharp cutoff is one of the most conventional choices in the NJL model studies. Because the sharp cutoff is incompatible with gauge invariance, a smooth cutoff such as the proper-time method [54] and the Pauli-Villars regularization would be more suitable for problems with electromagnetic background fields. For instance, in the derivations of the magnetic catalysis in Refs. [14, 15], the proper-time method was used to regularize the pure-magnetic potential (18).

As long as our main concern is about the magnetic catalysis, it is known that a naïve cutoff scheme would yield qualitatively correct results, as was also mentioned in Ref. [55] (see also Ref. [33] in which a naïve cutoff was adopted with the functional renormalization group equation). We note that the ultraviolet divergent structure is the same regardless of whether the system has rotation or not, apart from the ℓ -sum, so that we can use a naïve cutoff to find results that physically make sense. Then, to make the p_z -integral and the n -sum restricted in a region around $p_z^2 + 2neB \lesssim \Lambda^2$, we introduce a smoothed cutoff function as [55]

$$f(p_z, n; \Lambda) = \frac{\sinh(\Lambda/\delta\Lambda)}{\cosh[\tilde{\varepsilon}(p_z, n)\Lambda/\delta\Lambda] + \cosh(\Lambda/\delta\Lambda)} \quad (20)$$

with $\tilde{\varepsilon}\Lambda \equiv \sqrt{p_z^2 + 2neB}$. We note that in this function the smoothness to exclude artifacts is tuned by a parameter $\delta\Lambda$. Actually, in the $\delta\Lambda/\Lambda \rightarrow 0$ limit $f(p_z, n; \Lambda)$ is reduced to the step function $\theta(1 - \tilde{\varepsilon}) = \theta(\Lambda^2 - p_z^2 - 2neB)$. By changing $\delta\Lambda$ of such a simple function (20), we can systematically analyze whether our results are robust and not affected by cutoff artifact.

For the rest of this work we will focus on $m_{\text{current}} = T = 0$. The gap equation is the condition to minimize Eq. (17) with Eqs. (18) and (19). Then, we can write the gap equation down as follows:

$$\frac{m}{G} = \frac{m}{\pi} (F_0 - F_\Omega) \quad (21)$$

with the pure-magnetic term given by

$$F_0 \equiv \frac{eB}{2\pi} \sum_{n=0}^{\infty} \alpha_n \int_0^{\infty} \frac{dp_z f(p_z, n; \Lambda)}{\sqrt{p_z^2 + m_n^2}}, \quad (22)$$

and the rotational term given by

$$F_\Omega \equiv \frac{1}{S} \sum_{n=0}^{\infty} \alpha_n \sum_{\ell=-n}^{N-n} \theta(\Omega|j| - m_n) \int_0^{k_{nj}} \frac{dp_z f(p_z, n; \Lambda)}{\sqrt{p_z^2 + m_n^2}}. \quad (23)$$

This expression of F_Ω is slightly complicated for the evaluation. If k_{nj} is negligibly small compared with Λ and \sqrt{eB} , however, the rotational contribution F_Ω can be approximated with a simpler regularization by $f(0, n; \Lambda)$, which significantly simplifies the analytical treatment. Fortunately, this is the case for our analysis with a small

G (see Sec. IV A). In this approximation we can perform the p_z -integration in Eq. (23) analytically to reach:

$$F_\Omega \simeq \frac{1}{S} \sum_{n=0}^{\infty} \alpha_n \sum_{\ell=-n}^{N-n} \theta(\Omega|j| - m_n) f(0, n; \Lambda) \times \ln \left(\frac{\Omega|j| + \sqrt{(\Omega j)^2 - m_n^2}}{m_n} \right). \quad (24)$$

We note that we can immediately have the expression for finite-density systems by replacing F_Ω in Eq. (21) with

$$F_\mu = \frac{eB}{2\pi} \sum_{n=0}^{\infty} \alpha_n \theta(|\mu| - m_n) \ln \left(\frac{|\mu| + \sqrt{\mu^2 - m_n^2}}{m_n} \right), \quad (25)$$

which encompasses the mechanism for the inverse magnetic catalysis. It should be mentioned that we would not demand an ultraviolet regularization thanks to the step function, $\theta(|\mu| - m_n)$ in F_μ . From this, at the same time, we can understand that F_Ω is not really sensitive to the regularization scheme if S is large enough.

We should here refer to involved studies by Becattini *et al.* In Refs. [43], the quantum relativistic fermion system in rotating frame has been investigated in the aim of establishing a general thermodynamic and hydrodynamic framework to describe the system. Hence the chiral symmetry breaking has not been discussed. Also they have not considered the magnetic field which plays an important role to obviously show the analogy between rotation and density.

IV. NUMERICAL RESULTS AND DISCUSSIONS

In this section we analyse the magnetic response of the dynamical mass in rotating frames in the following two cases: (A) $G < G_c$ and (B) $G > G_c$, where G_c is the critical coupling for the onset of the chiral condensate in the vacuum (i.e. $\Omega = \sqrt{eB} = 0$)

$$G_c = 19.65/\Lambda^2, \quad (26)$$

which we numerically determined from Eqs. (21) using our present regulator (20) with

$$\delta\Lambda = 0.05\Lambda. \quad (27)$$

We have numerically verified that a different $\delta\Lambda$ would change the results quantitatively but the qualitative features are the same. For both (A) and (B) we choose the following parameters:

$$eB = (0.1 - 0.2)\Lambda^2, \\ S = 10^6 \pi / \Lambda^2 \quad (\text{i.e. } R = 10^3 / \Lambda). \quad (28)$$

We see that Eq. (14) is satisfied with the above parameter choice and the treatment of the Landau quantization is justified.

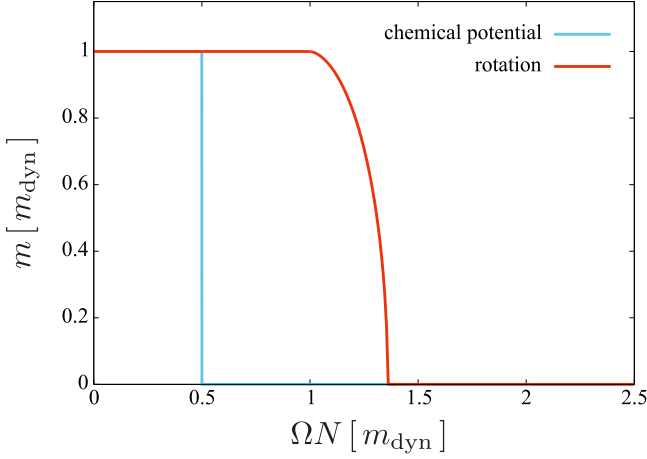


FIG. 1. Dynamical mass with $eB = 0.2\Lambda^2$ obtained from the gap equation (21) with rotation (red line) and with chemical potential $\mu = \mu_N$ (blue line). The model parameters are chosen as in Eq. (28).

A. Dynamical mass at weak coupling ($G < G_c$)

Let us discuss our numerical results with the following coupling:

$$G = 0.622G_c. \quad (29)$$

We define a unit of the dynamical mass as

$$m_{\text{dyn}} = 1.25 \times 10^{-2}\Lambda, \quad (30)$$

which is the solution of the gap equation with $eB = 0.2\Lambda^2$ and $\Omega = 0$. We show our numerical results in dimensionless unit in terms of m_{dyn} . In Fig. 1 we make a plot for the dynamical mass (red line) as a function of the angular velocity by solving Eq. (21) with rotation. The horizontal axis is given by an effective “chemical potential”:

$$\mu_N \equiv \Omega N. \quad (31)$$

In view of Eqs. (24) and (25) this ΩN is the maximum counterpart of μ .

To pursue the analogy between rotation and density quantitatively, we draw another (blue) line by solving the gap equation with F_Ω replaced with $F_\mu(\mu = \mu_N)$. Figure 2 is a 3D plot for the solution of Eq. (21) as a function of Ω and eB . We can observe that there is a threshold for the dynamical mass with increasing Ω , above which $m = 0$ and chiral symmetry is restored. This location of the critical Ω_c changes with eB , and we make Fig. 3 to show this eB -dependence of Ω_c . Here are some remarks on these numerical results.

(I) When the angular velocity exceeds $\Omega \simeq m_{\text{dyn}}/N$, the rotational effects become visible, but the damping of the dynamical mass starts slowly (see the red line in

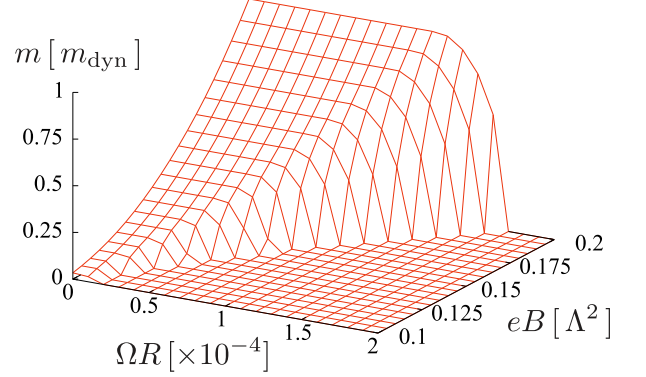


FIG. 2. 3D plot for the dynamical mass as a function of Ω and eB at weak coupling. For small Ω the dynamical mass grows exponentially with $1/eB$ (i.e. the magnetic catalysis). The critical Ω_c is also amplified exponentially as $1/eB$ decreases (see also Fig. 3).

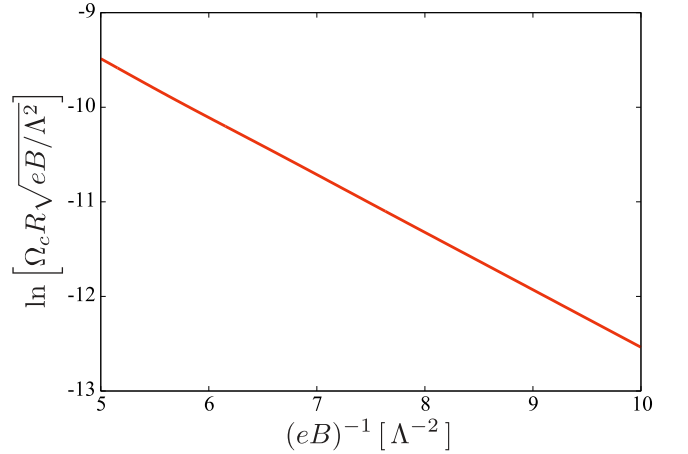


FIG. 3. eB -dependence of Ω_c for $0.1 \leq eB/\Lambda^2 \leq 0.2$. The linearity of $\ln \Omega_c$ vs $1/eB$ confirms the validity of the functional form of Ω_c given by Eq. (36).

Fig. 1). This behavior is different from the mass suppression induced by finite chemical potential (see the blue line in Fig. 1). Such a difference stems from the ℓ -dependence of each mode.

Let us count the number of modes that are relevant for the suppression of the dynamical mass. For simplicity, we concentrate only on the LLL with $n = 0$. In the present parameter choice, the LLL approximation should work well for F_Ω and F_μ . (The following argument should be also applicable even when higher Landau levels are not negligible.) Because of the step function in F_Ω , only the modes with $\ell > m/\Omega - 1/2$ give finite contributions. Indeed, the red line in Fig. 1 starts decreasing at $N\Omega \simeq m_{\text{dyn}}$, which corresponds to the threshold that

the highest angular momentum modes in F_Ω contributes nonvanishingly. In contrast, the step function in F_μ given in Eq. (25) indicates that all N modes simultaneously start contributing for $\mu > m$, while for $\mu < m$ nothing happens.

(II) Another way to investigate the difference between the red and the blue lines in Fig. 2 is to approximate the ℓ -sum. Suppose that Ω is small so that we can treat Ωj as a continuous variable. Also we assume a sufficiently large integer N . Then, we can approximate the ℓ -sum in F_Ω by an integration as

$$\begin{aligned} & \sum_{\ell=-n}^{N-n} \ln \left(\frac{\Omega|j| + \sqrt{(\Omega j)^2 - m_n^2}}{m_n} \right) \theta(\Omega|j| - m_n) \\ & \simeq \frac{1}{\Omega} \int_0^{\mu_N} d\mu \ln \left(\frac{\mu + \sqrt{\mu^2 - m_n^2}}{m_n} \right) \theta(\mu - m_n). \end{aligned} \quad (32)$$

For our parameter choice $N \sim \mathcal{O}(10^4)$ is large enough and the above approximation is justified. Then the rotational contribution to the gap equation (21) is reduced to

$$F_\Omega = F_\mu(\mu = \mu_N) - \frac{eB}{2\pi} \sum_{n=0}^{\infty} \alpha_n \sqrt{1 - \frac{m_n^2}{\mu_N^2}} \theta(\mu_N - m_n). \quad (33)$$

It is obvious that a density-like effect induced by rotation is certainly contained in the first term F_μ . The second is a negative term that makes a difference from the finite-density case. This extra term plays a role to weaken chiral restoration by rotation as compared to that by high density. Therefore, the suppression of the dynamical mass in the rotating frame occurs more gradually than that with the finite chemical potential. Moreover, Eq. (33) implies $F_\Omega < F_\mu$ for a fixed μ_N , and thus, chiral restoration by rotation would need larger μ_N than that by finite density (see Fig. 1).

(III) For $m_{\text{current}} = T = 0$ and large eB we can analytically investigate the eB -dependence of Ω_c . In our analysis we adopted the naïve cutoff regularization with Eq. (20), but the regularization scheme should be irrelevant for a large system with $S \gg 1/eB$. If we utilized the proper time regularization for F_0 , the gap equation with rotation and strong magnetic field would be [54]

$$\begin{aligned} \frac{4\pi^2}{G} &= \Lambda_{\text{PT}}^2 - m^2 \left[\ln \left(\frac{\Lambda_{\text{PT}}^2}{2eB} \right) - \gamma_E \right] \\ &+ eB \left[\ln \left(\frac{m^2}{4\pi eB} \right) + 2 \ln \Gamma \left(\frac{m^2}{2eB} \right) \right. \\ &\left. - 2 \ln \left(\frac{\mu_N + \sqrt{\mu_N^2 - m^2}}{m} \right) + 2 \sqrt{1 - \frac{m^2}{\mu_N^2}} \right], \end{aligned} \quad (34)$$

where γ_E is the Euler-Mascheroni constant, $\Gamma(z)$ denotes the gamma function, and Λ_{PT} stands for the cutoff parameter in the proper-time regularization. In this gap equation (34), the terms in the third line result from the

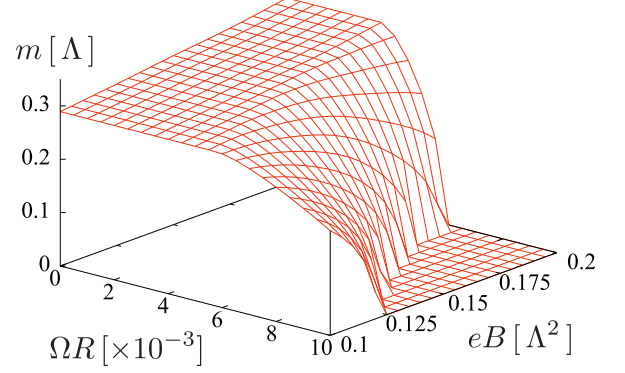


FIG. 4. 3D plot for the dynamical mass as a function of Ω and eB at strong coupling. For large Ω , chiral symmetry is restored by eB , which manifests the inverse magnetic catalysis or the rotational magnetic inhibition.

$n = 0$ mode in Eq. (33). We can find Ω_c from the above gap equation with $m \rightarrow 0$ substituted, and the analytical result is

$$\begin{aligned} \Omega_c(eB) &= \frac{\sqrt{\pi}}{S\sqrt{eB}} \exp \left[-\frac{2\pi^2}{eB} \left(\frac{1}{G} - \frac{1}{G_c} \right) + 1 \right] \\ &\simeq \frac{1.53 \times 10^{-6}}{\sqrt{eB}} \exp \left(-\frac{0.610\Lambda^2}{eB} \right), \end{aligned} \quad (35)$$

where $G_c = 4\pi/\Lambda_{\text{PT}}^2$ is the critical coupling for $\Omega = \sqrt{eB} = 0$ that is found in the proper-time regularization. In the second line in Eq. (35), we utilized the parameters of Eqs. (26), (29) and (28). On the other hand, we can numerically evaluate Ω_c as a function of eB as displayed in Fig. 3. From the linearity in Fig. 3 the numerical fit leads to

$$\Omega_c(eB) \simeq \frac{1.58 \times 10^{-6}}{\sqrt{eB}} \exp \left(-\frac{0.609\Lambda^2}{eB} \right). \quad (36)$$

This fitting result ensures that Eq. (32) is a good approximation for the parameters in Eq. (28).

B. Dynamical mass at strong coupling ($G > G_c$)

We shall next focus on the following strong region:

$$G = 1.11G_c. \quad (37)$$

We note that dynamically determined m with the above strong-coupling is about 20 times larger than m_{dyn} at weak coupling. We show the numerical results in Fig. 4. Below are several remarks on the results.

(I) For small angular velocity, the dynamical mass is almost independent of Ω and eB . With increasing Ω the

dynamical mass is eventually suppressed by larger magnetic field, i.e. a counterpart of the finite-density inverse magnetic catalysis is manifested. We would call this decreasing behavior of the mass for larger magnetic field the “rotational magnetic inhibition” in this paper. In Fig. 4 we see that the dynamical mass starts to drop around $\mu_N = \Omega N \sim \sqrt{eB}$. The same is true for the finite-density inverse magnetic catalysis observed around $\mu \sim \sqrt{eB}$ [30].

We notice that there is a drastic difference between the weak and the strong coupling results and this difference is attributed to higher Landau levels relevant for the determination of the dynamical mass. In the weak coupling case only a small number of the Landau levels contribute to the gap equation, while many more Landau levels get involved as the coupling constant becomes larger. This is essential for the realization of the rotational magnetic inhibition as well as of the inverse magnetic catalysis at finite density.

(II) Let us now take a close look at some possible difference between the finite-density inverse magnetic catalysis and the rotational magnetic inhibition. The QCD vacuum has a rich content with μ and eB , and for $G > G_c$, particularly, the de Haas-van Alphen oscillation [56] may lead to several local minima of the gap equation [17]. However, Fig. 4 shows that this is not the case for the rotational magnetic inhibition. To see the microscopic details, we should clarify the profile of the following function:

$$F(m) = \frac{1}{G} - \frac{1}{\pi}(F_0 - F_\Omega). \quad (38)$$

This function itself is continuous for any m , but the derivative is not, that is,

$$\begin{aligned} \frac{dF(m)}{dm} = & \frac{m}{\pi S} \sum_{n=0}^{\infty} \alpha_n \sum_{\ell=-n}^{N-n} \left[\int_0^\infty \frac{dp_z f(p_z, n; \Lambda)}{(p_z^2 + m_n^2)^{3/2}} \right. \\ & - \int_0^{k_{nj}} \frac{dp_z f(p_z, n; \Lambda)}{(p_z^2 + m_n^2)^{3/2}} \theta(\Omega|j| - m_n) \\ & \left. - \frac{f(\Omega|j|, 0; \Lambda)}{\Omega|j|\sqrt{(\Omega j)^2 - m_n^2}} \theta(\Omega|j| - m_n) \right], \end{aligned} \quad (39)$$

which negatively diverges at

$$m = \sigma_{nj} \equiv \sqrt{(\Omega j)^2 - 2neB}. \quad (40)$$

If m is greater than σ_{nj} , only the first term in the right-hand side of Eq. (39) remains nonvanishing for a fixed n , and we can confirm that Eq. (39) turns out to be positive. Thus, we find,

$$\left. \frac{dF(m)}{dm} \right|_{m \rightarrow \sigma_{nj}-0} = -\infty, \quad \left. \frac{dF(m)}{dm} \right|_{m \rightarrow \sigma_{nj}+0} > 0, \quad (41)$$

and so $F(m)$ may not be a monotonic function. This behavior in the vicinity of $m = \sigma_{nj}$ might cause technical

difficulties to deal with multiple zeros of $F(m)$. Indeed, a simple replacement of Ωj with μ leads to a profile of $F(m)$ having the de Haas-van Alphen oscillation for the mass gap [17, 34]. In the case with rotation, however, these singularities are not very important for the solution of the gap equation. In our numerical studies, actually, we find that $F(m)$ has only one solution, which is explained as follows.

If the effective chemical potential is not too large, i.e. $\mu_N = \Omega N \lesssim \Lambda$, we can practically remove the cutoff function from the third term in Eq. (39). Then we can approximate the ℓ -sum in the third term by an integration as we did in Eq. (32):

$$\begin{aligned} & \sum_{\ell=-n}^{N-n} \frac{1}{\Omega|j|\sqrt{(\Omega j)^2 - m_n^2}} \theta(\Omega|j| - m_n) \\ & \simeq \frac{1}{\Omega} \int_{m_n}^{\mu_N} \frac{d\mu}{\mu\sqrt{\mu^2 - m_n^2}} \theta(\mu_N - m_n) \\ & = \frac{1}{\Omega m_n} \left[\frac{\pi}{2} - \tan^{-1} \left(\frac{m_n}{\sqrt{\mu_N^2 - m_n^2}} \right) \right] \theta(\mu_N - m_n), \end{aligned} \quad (42)$$

which is finite even at $m = \sigma_{nN}$. In the opposite limit of large $\mu_N > \Lambda$, we can make a similar argument with μ_N replaced with Λ to confirm that no singularity appears from an approximated form of Eq. (39). Therefore, it is effectively possible for us to regard $F(m)$ as a monotonically increasing function in our numerical analysis. This explains why Fig. 4 does not show the de Haas-van Alphen oscillation.

(III) We briefly discuss the physical implications of the rotational magnetic inhibition to realistic situations at strong coupling (with chiral symmetry breaking in the vacuum). First, let us take an example from the condensed matter physics system; for a material with $R = 1$ cm (e.g. graphene or 3D Dirac semimetal) under the magnetic field $B = 1.7 \times 10^6$ G, we find that the rotational magnetic inhibition takes place around $\mu_N \sim \sqrt{eB}$, that is, $\Omega \sim \sqrt{eB}v_F/N \simeq 2.5 \times 10^2$ s⁻¹ where we adopt $v_F = 10^6$ m/s from the Fermi velocity of the quasiparticles in graphene [57]. This suggests that the rotational magnetic inhibition should be an observable effect in a table-top experiment.

Another interesting environment where the rotational magnetic inhibition could be activated is the neutron star. If one makes a naïve estimate for a millisecond pulsar, $\Omega \sim 10^3$ s⁻¹ and $R \sim 10^4$ m would lead to $\Omega R \sim \mathcal{O}(10^{-1})$. In view of Fig. 4 one may well conclude that chiral symmetry should be restored at small eB or even at zero eB . This is a very fascinating possibility that might have an impact to the construction of the equation of state (EoS); the neutron star EoS could get harder thanks to the rotational magnetic inhibition. We have to leave quantitative studies for future works, however, because $R \simeq 10^4$ m is outside of the region of R that we adopted in this paper. Here we just emphasize

that due to the quadratic dependence, $\mu_N \propto R^2$, the chiral condensate with larger R is generally more sensitive to the rotational effect. Thus, the rotational magnetic inhibition must be definitely a sizable effect for the neutron star physics.

V. CONCLUSION AND OUTLOOK

We analyzed the Dirac equation with magnetic field background in a rotating frame. We showed that rotation should modify the Landau levels and resolve the Landau degeneracy. As a result, rotation plays a role similar with finite chemical potential. In the weak coupling case where chiral symmetry is not yet broken in the vacuum, the dynamical mass is induced by the magnetic field according to the well-known magnetic catalysis. Together with rotation, we found that the dynamical mass is suppressed with increasing angular velocity Ω . For strong coupling case that realizes chiral symmetry breaking in the vacuum, we discovered opposite behavior of the dynamical mass. At finite Ω (like finite density), the dynamical mass decreases with increasing magnetic field. This phenomenon is an inverse of the conventional magnetic catalysis, and could be regarded as an example of the inverse magnetic catalysis. To distinguish our finding from the inverse magnetic catalysis at finite density or finite temperature, we named this novel phenomenon the “rotational magnetic inhibition.”

We should note that the rotational responses obtained from our calculation are model-independent. We introduced a specific cutoff function for the p_z -integral and the n -sum to evaluate the chiral condensate within the NJL model. Nevertheless, we also confirmed that the behaviors of the chiral condensate are qualitatively unchanged even if we use other parameters. Additionally once we regularize the n -sum, the upper bound of angular momentum ℓ is automatically determined by the Landau degeneracy factor, which is irrelevant to model parameters. Thus whatever model and parameters we adopt, rotation should give density-like contributions to the dynamical mass, as expected in the level of the energy spectrum.

We can find many possible applications of the rotational magnetic inhibition. We could discuss it in condensed matter systems, in the cores of the neutron star, and in noncentral relativistic heavy-ion collision experiments [58]. We gave a rough estimate of whether our analysis could be relevant for those systems. For the heavy-ion collision the estimate of Ω is still unclear and it is difficult to make any decisive statement. For the neutron star, although angular velocity itself is much smaller than the QCD scale, it is obvious from our results that the rotation should give a sizable modification to the dynamical mass through an effective chemical potential $\mu_N = \Omega N$. Hence we must consider the rotational influence to the equation of state (EoS); so far, its angular velocity seems too small to affect the QCD dynamics

and the rotation has been treated only as a global effect in the EoS [59] (see also Refs. [60–63]). We are now making a progress to go beyond such a treatment.

To this end, though it is beyond our scope of the present paper, we would need to consider spatially inhomogeneous condensates as done in finite-density systems (see Ref. [64] and references therein) together with a magnetic field [65, 66] and also in systems influenced by surrounding geometrical effects [46, 47]. Most probably the chiral condensate could be decreasing as the radial distance from the rotation center becomes larger. In the present analysis we assumed a homogeneous condensate using not the effective action but the effective potential only. This is how the results depend on the bulk parameter R , which might be augmented with local radial distance dependence. The main purpose of this current study is to pursue the analogy between rotation and density and we would leave more quantitative discussions including spatial inhomogeneity for future works.

ACKNOWLEDGMENTS

This work was supported by Japan Society for the Promotion of Science (JSPS) KAKENHI Grant No. 15H03652 and 15K13479 (K. F.), JSPS Research Fellowships for Young Scientists (K. M.), and Shanghai Natural Science Foundation (Grant No. 14ZR1403000) and the Young 1000 Talents Program of China (H.-L. C. and X.-G. H).

Appendix A: Dirac equation in a rotating frame

We solve the Dirac equation in a rotating frame (5). We find that the quantum number ℓ in Eq. (8) is same as that without rotation. We also show that a quite large system size as Eq. (14) is necessary for the Landau quantization.

We rewrite Eq. (5) as the following equation:

$$\begin{aligned}
 0 &= [i\gamma^\mu(D_\mu + \Gamma_\mu) + m][i\gamma^\mu(D_\mu + \Gamma_\mu) - m]\psi \\
 &= \left[(i\partial_t + \Omega\hat{L}_z + \Omega\sigma^{12})^2 + \partial_x^2 + \partial_y^2 + \partial_z^2 \right. \\
 &\quad \left. + eB(\hat{L}_z + 2\sigma^{12}) - \left(\frac{eB}{2}\right)^2(x^2 + y^2) - m^2 \right] \psi \quad (\text{A1}) \\
 &= \left[(i\partial_t - i\Omega\partial_\theta + \Omega\sigma^{12})^2 + \partial_r^2 + \frac{1}{r}\partial_r + \frac{1}{r^2}\partial_\theta^2 \right. \\
 &\quad \left. + eB(-i\partial_\theta + 2\sigma^{12}) - \left(\frac{eB}{2}\right)^2 r^2 + \partial_z^2 - m^2 \right] \psi.
 \end{aligned}$$

The last line is written with the cylindrical coordinate $x^\mu = (t, r, \theta, z)$. Taking the chiral representation

$$\psi = \begin{pmatrix} \chi \\ \varphi \end{pmatrix}, \quad (\text{A2})$$

the solution is written as the following function:

$$\chi = e^{-iEt+ip_z z} \begin{pmatrix} e^{i\ell_+\theta} \chi_+(r) \\ e^{i\ell_-\theta} \chi_-(r) \end{pmatrix}, \quad (\text{A3})$$

where ℓ_\pm is an integer and the radial function is defined as $\sigma^3 \chi_\pm = \pm \chi_\pm$. In what follows, we solve only the equation of χ , but that of φ can be solved in the same way. Because of the rotational invariance, ψ should also be an eigenfunction for $\hat{J}_z = \hat{L}_z + \sigma^{12}$. In other words, χ_\pm have equivalent total angular momenta, which leads

$$\ell_+ = \ell_- - 1. \quad (\text{A4})$$

We note that at this stage, there are no constraint for ℓ_\pm other than Eq. (A4).

Substituting ψ with Eq. (A2), we obtain the equation for χ_\pm :

$$\left[\left\{ E + \Omega(\ell_\pm \pm 1/2) \right\}^2 - p_z^2 - m^2 + eB(\ell_\pm \pm 1) + \partial_r^2 + \frac{1}{r} \partial_r - \frac{\ell_\pm^2}{r^2} - \left(\frac{eB}{2} \right)^2 r^2 \right] \chi_\pm = 0. \quad (\text{A5})$$

The solution for this equation is written with the confluent hypergeometric function:

$$\chi_\pm = r^{|\ell_\pm|} e^{-eBr^2/4} \left[c_1 M(a, |\ell_\pm| + 1, eBr^2/2) + c_2 (eBr^2/2)^{-|\ell_\pm|} M(a - |\ell_\pm|, 1 - |\ell_\pm|, eBr^2/2) \right] \quad (\text{A6})$$

with

$$a = \frac{1}{2} (|\ell_\pm| \mp 1 - \ell_\pm + 1) - \frac{1}{2eB} \left[\left\{ E + \Omega(\ell_\pm \pm 1/2) \right\}^2 - p_z^2 - m^2 \right]. \quad (\text{A7})$$

It is necessary that χ_\pm be finite at arbitrary r because of normalizability. The finiteness of $\chi_\pm(r \rightarrow 0)$ demands $c_2 = 0$. Also to keep $\chi_\pm(r \rightarrow \infty)$ finite, a should be a nonpositive integer:

$$-a \equiv n_p = 0, 1, 2, \dots \quad (\text{A8})$$

In this case, this hypergeometric function is reduced to an associated Laguerre polynomial:

$$M(-n_p, |\ell_\pm| + 1, eBr^2/2) = C_{n,|\ell_\pm|} L_{n_p}^{|\ell_\pm|}(eBr^2/2), \quad (\text{A9})$$

where $C_{n,|\ell_\pm|}$ is a constant independent of r . From Eq. (A8), we find that the energy dispersion relation is quantized:

$$\left[E + \Omega(\ell_\pm \pm 1/2) \right]^2 = eB(2n_p + |\ell_\pm| - \ell_\pm + 1 \mp 1) + p_z^2 + m^2. \quad (\text{A10})$$

This dispersion can be reduced to Eq. (8) if we introduce the new integers defined by

$$\begin{aligned} n &= n_+ = n_- + 1, \\ n_\pm &\equiv n_p + \frac{1}{2} (|\ell_\pm| - \ell_\pm + 1 \mp 1). \end{aligned} \quad (\text{A11})$$

We note that these equations imply the lower bounds for ℓ_\pm :

$$\ell \equiv \ell_+ = \ell_- - 1 \geq -n. \quad (\text{A12})$$

Finally using the property of the Laguerre function,

$$L_{n+\ell}^{-\ell}(x^2) \propto x^{2\ell} L_n^\ell(x^2) \quad (\text{for } \ell \leq 0), \quad (\text{A13})$$

we obtain the eigenfunction as the following simpler form:

$$\chi_{n,\ell,\pm}(r) \propto r^\ell e^{-eBr^2/4} L_n^\ell(eBr^2/2). \quad (\text{A14})$$

We mention that the above argument is valid even in the $\Omega = 0$ case. This means that the quantum number ℓ is the same as the one without rotation. Therefore the possible range of ℓ in a rotating frame is same as the one without rotation, i.e., Eq. (12) (see Appendix B).

For the discussion in this paper, it is significant that the quantization in terms of n_p in Eq. (A8) is performed only if the wave function converges at infinity. The same is true for the quantization of general harmonic oscillators. This is why we need to consider systems with a much larger radius than $\ell_B = 1/\sqrt{eB}$, as shown in Eq. (14).

Appendix B: Landau degeneracy in cylinders

Based on the Klein–Gordon equation for charged scalar in external magnetic field, we briefly show that even in cylindrical coordinate the Landau degeneracy factor is given by Eq. (11), as well as in Cartesian coordinate. It is also proved that the range of quantum number ℓ for the n th Landau level is given by Eq. (12).

1. Landau quantization for general gauges

We prepare the Landau quantization for general gauge. The Klein-Gordon equation in a magnetic field $\mathbf{B} = B\hat{z}$ is as follows:

$$(\partial_t^2 - \partial_z^2 + m^2 - D_x^2 - D_y^2)\Phi = 0. \quad (\text{B1})$$

It is clear that the solution is the form given by $\Phi = e^{-i\epsilon t + ikz} \phi(x, y)$. The Klein–Gordon equation is then reduced to

$$\hat{H}\phi(x, y) = \lambda\phi(x, y) \quad (\text{B2})$$

with

$$\hat{H} \equiv -(D_x^2 + D_y^2), \quad \lambda \equiv \varepsilon^2 - k^2 - m^2. \quad (\text{B3})$$

This eigenvalue equation can be solved by introducing the ladder operators:

$$a \equiv \frac{i}{\sqrt{2eB}}(D_x + iD_y), \quad a^\dagger \equiv \frac{i}{\sqrt{2eB}}(D_x - iD_y), \quad (\text{B4})$$

which satisfy $[a, a^\dagger] = 1$. Therefore the eigenstates for Eq. (B2) are $|n\rangle \propto (a^\dagger)^n |0\rangle$, and the corresponding eigenvalue is given by

$$\hat{H}|n\rangle = eB(2n+1)|n\rangle. \quad (\text{B5})$$

2. Landau quantization for symmetric gauge

When we utilize the cylindrical coordinate, the symmetric gauge $A_\mu = (0, By/2, -Bx/2, 0)$ is most useful because the Hamiltonian in Eq. (B2) respects the rotational symmetry. Instead of (r, θ) , we use the complex coordinate defined by

$$z \equiv x + iy, \quad \bar{z} \equiv x - iy. \quad (\text{B6})$$

We also introduce the new notations for the derivatives in terms of z and \bar{z} : $\partial \equiv \partial/\partial z$ and $\bar{\partial} \equiv \partial/\partial \bar{z}$. Then the ladder operators are also rewritten by (z, \bar{z}) :

$$a = \frac{-i}{\sqrt{2eB}} \left(2\bar{\partial} + \frac{eB}{2} z \right), \quad a^\dagger = \frac{-i}{\sqrt{2eB}} \left(2\partial - \frac{eB}{2} \bar{z} \right). \quad (\text{B7})$$

The ground state is obtained by the condition $a|0\rangle = 0$:

$$\langle z, \bar{z} | a | 0 \rangle = -i \frac{1}{\sqrt{2eB}} \left(2\bar{\partial} + \frac{eB}{2} z \right) \phi(z, \bar{z}) = 0. \quad (\text{B8})$$

The solution is given by

$$\phi(z, \bar{z}) = \tilde{\phi}(z) e^{-eBz\bar{z}/4}, \quad (\text{B9})$$

where $\tilde{\phi}(z)$ denotes a function of z . In principle, we have no condition for the choice of $\tilde{\phi}(z)$, except for the analyticity. This facultativity of $\tilde{\phi}(z)$ comes from assuming an infinitely large system in our calculation. In other words, the eigenvalue equation of the harmonic oscillator cannot be solved in finite-size systems (see Appendix A).

In order to find $\tilde{\phi}(z)$, we analyze another quantum number, i.e., the canonical angular momentum. Because of the rotational-invariance of the Hamiltonian, the eigenstate of the Hamiltonian can be also the eigenstate of the angular momentum $\hat{L}_z = xp_y - yp_x = z\partial - \bar{z}\bar{\partial}$. Let us introduce the new ladder operators:

$$b \equiv \frac{1}{\sqrt{2eB}} \left(2\partial + \frac{eB}{2} \bar{z} \right), \quad b^\dagger \equiv \frac{1}{\sqrt{2eB}} \left(-2\bar{\partial} + \frac{eB}{2} z \right), \quad (\text{B10})$$

which satisfy $[b, b^\dagger] = 1$. We represent the angular momentum as the ladder operators:

$$\hat{L}_z = b^\dagger b - a^\dagger a. \quad (\text{B11})$$

We define the simultaneous eigenstates for $a^\dagger a$ and $b^\dagger b$:

$$a^\dagger a |n, n_p\rangle = n |n, n_p\rangle, \quad b^\dagger b |n, n_p\rangle = n_p |n, n_p\rangle, \quad (\text{B12})$$

for $n, n_p = 0, 1, \dots$. Instead of n_p , we designate these eigenstates by the new quantum number $\ell = n_p - n$:

$$\begin{aligned} \langle z, \bar{z} | n, n_p \rangle &= \phi_{nn_p}(z, \bar{z}) \equiv \psi_{n\ell}(z, \bar{z}), \\ \hat{L}_z \psi_{n\ell} &= (b^\dagger b - a^\dagger a) \psi_{n\ell} = \ell \psi_{n\ell}. \end{aligned} \quad (\text{B13})$$

We note that the non-negativities of n and n_p lead to the lower bound of ℓ :

$$\ell \geq -n. \quad (\text{B14})$$

We produce a ground state by the operation of ladder operator b^\dagger :

$$\begin{aligned} \psi_{0\ell}(z, \bar{z}) &\propto (b^\dagger)^\ell \psi_{00}(z, \bar{z}) \\ &\propto z^\ell e^{-eBz\bar{z}/4}. \end{aligned} \quad (\text{B15})$$

From this eigenstate, we find that ℓ corresponds to the degenerate quantum number, which is irrelevant to the energy level. Thus the possible range of ℓ is nothing but the Landau degeneracy factor. In order to calculate the degeneracy factor, we focus on the following equation:

$$\frac{d}{dr} (2\pi r |\psi_{0\ell}|^2) = 0, \quad (\text{B16})$$

which determines the radius that gives the maximum value of this distribution. If we consider the system to be the cylinder with radius R , the solution for Eq. (B16) should be smaller than R , which leads to the upper bound of ℓ :

$$\ell \leq \frac{eBR^2}{2} = \frac{eBS}{2\pi}. \quad (\text{B17})$$

Therefore from this upper bound and the lower bound $\ell \geq -n = 0$, the degeneracy factor in the cylindrical coordinate is given by Eq. (11).

Higher excited states with $n \geq 1$ are calculated in a similar way to ground states:

$$\begin{aligned} \psi_{n\ell}(z, \bar{z}) &\propto (a^\dagger)^n (b^\dagger)^{n+\ell} \psi_{00}(z, \bar{z}) \\ &\propto z^\ell e^{-eBz\bar{z}/4} L_n^\ell(eBz\bar{z}/2), \end{aligned} \quad (\text{B18})$$

which is same as Eq. (A14) if we use $z = re^{i\theta}$ and $\bar{z} = re^{-i\theta}$. The upper bound of ℓ for excited states cannot directly be found from Eq. (B18) while the one for the ground state is derived from the wave function (B15). Nevertheless the upper bound of ℓ for excited states is obviously $N - n$ because the degeneracy factor N is a common quantity for all Landau levels. From this and the lower bound $\ell \geq -n$, we obtain Eq. (12).

-
- [1] B.-l. Cheng and A. V. Olinto, *Phys. Rev.* **D50**, 2421 (1994); G. Baym, D. Bodeker, and L. D. McLerran, *Phys. Rev.* **D53**, 662 (1996), [arXiv:hep-ph/9507429 \[hep-ph\]](#).
- [2] D. Grasso and H. R. Rubinstein, *Phys. Rept.* **348**, 163 (2001), [arXiv:astro-ph/0009061 \[astro-ph\]](#).
- [3] R. C. Duncan and C. Thompson, *Astrophys. J.* **392**, L9 (1992).
- [4] V. Skokov, A. Yu. Illarionov, and V. Toneev, *Int. J. Mod. Phys.* **A24**, 5925 (2009), [arXiv:0907.1396 \[nucl-th\]](#).
- [5] V. Voronyuk, V. D. Toneev, W. Cassing, E. L. Bratkovskaya, V. P. Konchakovski, and S. A. Voloshin, *Phys. Rev.* **C83**, 054911 (2011), [arXiv:1103.4239 \[nucl-th\]](#).
- [6] W.-T. Deng and X.-G. Huang, *Phys. Rev.* **C85**, 044907 (2012), [arXiv:1201.5108 \[nucl-th\]](#).
- [7] N. Brambilla *et al.*, *Eur. Phys. J.* **C74**, 2981 (2014), [arXiv:1404.3723 \[hep-ph\]](#).
- [8] D. Kharzeev and A. Zhitnitsky, *Nucl. Phys.* **A797**, 67 (2007), [arXiv:0706.1026 \[hep-ph\]](#); D. E. Kharzeev, L. D. McLerran, and H. J. Warringa, *Nucl. Phys.* **A803**, 227 (2008), [arXiv:0711.0950 \[hep-ph\]](#); K. Fukushima, D. E. Kharzeev, and H. J. Warringa, *Phys. Rev.* **D78**, 074033 (2008), [arXiv:0808.3382 \[hep-ph\]](#).
- [9] D. T. Son and A. R. Zhitnitsky, *Phys. Rev.* **D70**, 074018 (2004), [arXiv:hep-ph/0405216 \[hep-ph\]](#).
- [10] M. A. Metlitski and A. R. Zhitnitsky, *Phys. Rev.* **D72**, 045011 (2005), [arXiv:hep-ph/0505072 \[hep-ph\]](#).
- [11] D. T. Son and P. Surowka, *Phys. Rev. Lett.* **103**, 191601 (2009), [arXiv:0906.5044 \[hep-th\]](#).
- [12] D. E. Kharzeev and H.-U. Yee, *Phys. Rev.* **D83**, 085007 (2011), [arXiv:1012.6026 \[hep-th\]](#).
- [13] K. Fukushima, *Lect. Notes Phys.* **871**, 241 (2013), [arXiv:1209.5064 \[hep-ph\]](#); D. E. Kharzeev, *Prog. Part. Nucl. Phys.* **75**, 133 (2014), [arXiv:1312.3348 \[hep-ph\]](#); X.-G. Huang, (2015), [arXiv:1509.04073 \[nucl-th\]](#); D. E. Kharzeev, J. Liao, S. A. Voloshin, and G. Wang, (2015), [arXiv:1511.04050 \[hep-ph\]](#).
- [14] K. G. Klimenko, *Z. Phys.* **C54**, 323 (1992); *Theor. Math. Phys.* **90**, 1 (1992), [*Teor. Mat. Fiz.*90,3(1992)].
- [15] V. P. Gusynin, V. A. Miransky, and I. A. Shovkovy, *Phys. Rev. Lett.* **73**, 3499 (1994), [Erratum: *Phys. Rev. Lett.*76,1005(1996)], [arXiv:hep-ph/9405262 \[hep-ph\]](#); *Nucl. Phys.* **B462**, 249 (1996), [arXiv:hep-ph/9509320 \[hep-ph\]](#).
- [16] I. A. Shovkovy, *Lect. Notes Phys.* **871**, 13 (2013), [arXiv:1207.5081 \[hep-ph\]](#); V. A. Miransky and I. A. Shovkovy, *Phys. Rept.* **576**, 1 (2015), [arXiv:1503.00732 \[hep-ph\]](#).
- [17] D. Ebert, K. G. Klimenko, M. A. Vdovichenko, and A. S. Vshivtsev, *Phys. Rev.* **D61**, 025005 (1999), [arXiv:hep-ph/9905253 \[hep-ph\]](#).
- [18] T. Inagaki, D. Kimura, and T. Murata, *Prog. Theor. Phys.* **111**, 371 (2004), [arXiv:hep-ph/0312005 \[hep-ph\]](#).
- [19] E. S. Fraga and A. J. Mizher, *Phys. Rev.* **D78**, 025016 (2008), [arXiv:0804.1452 \[hep-ph\]](#).
- [20] A. J. Mizher, M. N. Chernodub, and E. S. Fraga, *Phys. Rev.* **D82**, 105016 (2010), [arXiv:1004.2712 \[hep-ph\]](#).
- [21] J. O. Andersen and R. Khan, *Phys. Rev.* **D85**, 065026 (2012), [arXiv:1105.1290 \[hep-ph\]](#).
- [22] G. N. Ferrari, A. F. Garcia, and M. B. Pinto, *Phys. Rev.* **D86**, 096005 (2012), [arXiv:1207.3714 \[hep-ph\]](#).
- [23] E. S. Fraga and L. F. Palhares, *Phys. Rev.* **D86**, 016008 (2012), [arXiv:1201.5881 \[hep-ph\]](#).
- [24] G. S. Bali, F. Bruckmann, G. Endrodi, Z. Fodor, S. D. Katz, and A. Schafer, *Phys. Rev.* **D86**, 071502 (2012), [arXiv:1206.4205 \[hep-lat\]](#).
- [25] C. V. Johnson and A. Kundu, *JHEP* **12**, 053 (2008), [arXiv:0803.0038 \[hep-th\]](#).
- [26] E. V. Gorbar, V. P. Gusynin, and V. A. Miransky, *Low Temp. Phys.* **34**, 790 (2008), [arXiv:0710.3527 \[cond-mat.mes-hall\]](#); E. V. Gorbar, V. P. Gusynin, V. A. Miransky, and I. A. Shovkovy, *Phys. Rev.* **B78**, 085437 (2008), [arXiv:0806.0846 \[cond-mat.mes-hall\]](#).
- [27] B. Roy and J. D. Sau, *Phys. Rev.* **B92**, 125141 (2015), [arXiv:1406.4501 \[cond-mat.mes-hall\]](#).
- [28] A. Ayala, M. Loewe, J. C. Rojas, and C. Villavicencio, *Phys. Rev.* **D86**, 076006 (2012), [arXiv:1208.0390 \[hep-ph\]](#).
- [29] B. Feng, D.-F. Hou, and H.-C. Ren, *Phys. Rev.* **D92**, 065011 (2015), [arXiv:1412.1647 \[cond-mat.quant-gas\]](#).
- [30] F. Preis, A. Rebhan, and A. Schmitt, *JHEP* **03**, 033 (2011), [arXiv:1012.4785 \[hep-th\]](#).
- [31] K. Fukushima and Y. Hidaka, *Phys. Rev. Lett.* **110**, 031601 (2013), [arXiv:1209.1319 \[hep-ph\]](#).
- [32] G. S. Bali, F. Bruckmann, G. Endrodi, Z. Fodor, S. D. Katz, S. Krieg, A. Schafer, and K. K. Szabo, *JHEP* **02**, 044 (2012), [arXiv:1111.4956 \[hep-lat\]](#).
- [33] K. Fukushima and J. M. Pawłowski, *Phys. Rev.* **D86**, 076013 (2012), [arXiv:1203.4330 \[hep-ph\]](#).
- [34] F. Preis, A. Rebhan, and A. Schmitt, *Lect. Notes Phys.* **871**, 51 (2013), [arXiv:1208.0536 \[hep-ph\]](#).
- [35] F. Bruckmann, G. Endrodi, and T. G. Kovacs, *JHEP* **04**, 112 (2013), [arXiv:1303.3972 \[hep-lat\]](#).
- [36] N. K. Wilkin and J. M. F. Gunn, *Phys. Rev. Lett.* **84**, 6 (2000); N. R. Cooper, N. K. Wilkin, and J. M. F. Gunn, *Phys. Rev. Lett.* **87**, 120405 (2001); V. Schweikhard, I. Coddington, P. Engels, V. P. Møgelgaard, and E. A. Cornell, *Phys. Rev. Lett.* **92**, 040404 (2004), [arXiv:cond-mat/0308582 \[cond-mat.mes-hall\]](#).
- [37] K. Mameda and A. Yamamoto, (2015), [arXiv:1504.05826 \[hep-th\]](#).
- [38] S. Viefers, *J. of Phys.: Cond. Matt.* **20**, 123202 (2008).
- [39] M. Tsubota, K. Kasamatsu, and M. Kobayashi, *Novel Superfluids: Volume 1* (Oxford University Press, 2013).
- [40] X.-G. Huang, (2015), [arXiv:1506.03590 \[cond-mat.quant-gas\]](#).
- [41] L. Parker and D. Toms, *Quantum field theory in curved spacetime: quantized fields and gravity* (Cambridge University Press, 2009).
- [42] F. Becattini and L. Ferroni, *Eur. Phys. J.* **C52**, 597 (2007), [arXiv:0707.0793 \[nucl-th\]](#).
- [43] F. Becattini and F. Piccinini, *Annals Phys.* **323**, 2452 (2008), [arXiv:0710.5694 \[nucl-th\]](#); F. Becattini and L. Tinti, *Annals Phys.* **325**, 1566 (2010), [arXiv:0911.0864 \[gr-qc\]](#); F. Becattini, V. Chandra, L. Del Zanna, and E. Grossi, *Annals Phys.* **338**, 32 (2013), [arXiv:1303.3431 \[nucl-th\]](#).
- [44] E. Elizalde, S. Leseduarte, and S. D. Odintsov, *Phys. Rev.* **D49**, 5551 (1994), [arXiv:hep-th/9312164 \[hep-th\]](#); T. Inagaki, T. Muta, and S. D. Odintsov, *Mod. Phys. Lett.* **A08**, 2117 (1993), [arXiv:hep-th/9306023 \[hep-th\]](#).

- Prog. Theor. Phys. Suppl. **127**, 93 (1997), [arXiv:hep-th/9711084 \[hep-th\]](#); E. V. Gorbar, *Phys. Rev.* **D61**, 024013 (1999), [arXiv:hep-th/9904180 \[hep-th\]](#); X.-G. Huang, X.-W. Hao, and P.-F. Zhuang, *Astropart. Phys.* **28**, 472 (2007), [arXiv:hep-ph/0602186 \[hep-ph\]](#).
- [45] R. Schutzhold, *Phys. Rev. Lett.* **89**, 081302 (2002), [arXiv:gr-qc/0204018 \[gr-qc\]](#); F. R. Urban and A. R. Zhitnitsky, *Nucl. Phys.* **B835**, 135 (2010), [arXiv:0909.2684 \[astro-ph.CO\]](#).
- [46] A. Flachi and T. Tanaka, *Phys. Rev.* **D84**, 061503 (2011), [arXiv:1106.3991 \[hep-th\]](#); A. Flachi, *Phys. Rev.* **D88**, 041501 (2013), [arXiv:1305.5348 \[hep-th\]](#); A. Flachi and K. Fukushima, *Phys. Rev. Lett.* **113**, 091102 (2014), [arXiv:1406.6548 \[hep-th\]](#).
- [47] S. Benic and K. Fukushima, (2015), [arXiv:1503.05790 \[hep-th\]](#).
- [48] A. Yamamoto and Y. Hirono, *Phys. Rev. Lett.* **111**, 081601 (2013), [arXiv:1303.6292 \[hep-lat\]](#).
- [49] A. Yamamoto, *Phys. Rev.* **D90**, 054510 (2014), [arXiv:1405.6665 \[hep-lat\]](#).
- [50] S. Benic and A. Yamamoto, (2016), [arXiv:1603.00716 \[hep-lat\]](#).
- [51] P. C. W. Davies, T. Dray, and C. A. Manogue, *Phys. Rev.* **D53**, 4382 (1996), [arXiv:gr-qc/9601034 \[gr-qc\]](#).
- [52] G. Duffy and A. C. Ottewill, *Phys. Rev.* **D67**, 044002 (2003), [arXiv:hep-th/0211096 \[hep-th\]](#).
- [53] Y. Nambu and G. Jona-Lasinio, *Phys. Rev.* **122**, 345 (1961).
- [54] J. S. Schwinger, *Phys. Rev.* **82**, 664 (1951).
- [55] E. V. Gorbar, V. A. Miransky, and I. A. Shovkovy, *Phys. Rev.* **D83**, 085003 (2011), [arXiv:1101.4954 \[hep-ph\]](#).
- [56] W. De Haas and P. van Alphen, in *Proc. Netherlands Roy. Acad. Sci*, Vol. 33 (1930) p. 170; W. De Haas and P. Van Alphen, *Leiden Commun* **208**, 212a (1930).
- [57] K. S. Novoselov, A. K. Geim, S. V. Morozov, D. Jiang, M. I. Katsnelson, I. V. Grigorieva, S. V. Dubonos, and A. A. Firsov, *Nature* **438**, 197 (2005), [arXiv:cond-mat/0509330 \[cond-mat.mes-hall\]](#).
- [58] L. P. Csernai, V. K. Magas, H. Stocker, and D. D. Strottman, *Phys. Rev.* **C84**, 024914 (2011), [arXiv:1101.3451 \[nucl-th\]](#).
- [59] G. B. Cook, S. L. Shapiro, and S. A. Teukolsky, *Astrophys. J.* **424**, 823 (1994).
- [60] J. Friedman, J. Ipser, and L. Parker, *The Astrophysical Journal* **304**, 115 (1986).
- [61] N. K. Glendenning, S. Pei, and F. Weber, *Phys. Rev. Lett.* **79**, 1603 (1997).
- [62] E. Chubarian, H. Grigorian, G. Poghosyan, and D. Blaschke, (1999), [arXiv:astro-ph/9903489 \[astro-ph\]](#).
- [63] P. Haensel, A. Y. Potekhin, and D. G. Yakovlev, *Neutron stars 1: Equation of state and structure*, Vol. 326 (Springer Science & Business Media, 2007).
- [64] M. Buballa and S. Carignano, *Prog. Part. Nucl. Phys.* **81**, 39 (2015), [arXiv:1406.1367 \[hep-ph\]](#).
- [65] K. Fukushima and P. A. Morales, *Phys. Rev. Lett.* **111**, 051601 (2013), [arXiv:1305.4115 \[hep-ph\]](#).
- [66] S. Carignano, E. J. Ferrer, V. de la Incera, and L. Paulucci, *Phys. Rev.* **D92**, 105018 (2015), [arXiv:1505.05094 \[nucl-th\]](#).